Open access • Journal Article • DOI:10.1103/PHYSREVA.51.1420

Monte Carlo classical simulations of ionization and harmonic generation in the relativistic domain. — Source link

Christoph H. Keitel, Peter L. Knight

Institutions: Max Planck Society, Imperial College London

Published on: 01 Feb 1995 - Physical Review A (Published by the American Physical Society through the American Institute of Physics)

Topics: High harmonic generation, Ionization, Monte Carlo method, Harmonics and Field (physics)

Monte Carlo classical simulations of ionization and harmonic generation in the relativistic domain

C. H. Keitel and P. L. Knight
Optics Section, Blackett Laboratory, Imperial College, London SW7 2BZ, United Kingdom
(Received 18 July 1994)

The magnetic-field component of a very intense laser field interacting with an atom cannot normally be neglected for intensities that lead to relativistic velocities of the electrons. Here we investigate stabilization and harmonic generation in this relativistic regime from a three-dimensional hydrogen atom modeled as a classical system with a distribution of initial conditions derived from a Monte Carlo average. Particular emphasis is placed on the problems of ionization in the direction of propagation of the applied laser field, which will be shown to arise from the inclusion of the magnetic-field component of the laser field. In the harmonic spectra, Doppler shifting occurs for observation directions orthogonal to the direction of laser-field propagation. Retardation effects show up in the harmonic spectra in the forward direction and inhibit the magnetic-field effects of the free-electron contribution of the forward-direction spectrum. In general, few harmonics are observed in our single-atom treatment because of the magnetically induced three-dimensional motion of the electron for intensities approaching the relativistic regime, and because of high ionization probabilities, i.e., also the breakdown of stabilization, for strongly relativistic laser intensities.

PACS number(s): 32.80.Rm, 42.50.Hz, 42.65.Ky

I. INTRODUCTION

The idea of generating high-frequency radiation through up-conversion of fundamental laser frequencies by inducing atoms to emit high multiples (harmonics) of an applied intense laser field has always appeared particularly useful [1–5]. Recent progress in short pulse laser technology has achieved laser-field intensities which impose electric forces on the electron which exceed those of the binding nucleus. Under these conditions, the strongly accelerated electron is found to radiate very high harmonics, up to the 165th being observed [6–9], and this is understood to happen when the electron wave packet approaches the vicinity of the nucleus [10].

Due to the crucial role of the nucleus, much effort has been put into understanding the problem of ionization (the ejection of the electron) in the polarization direction of the laser field, which can already hamper high harmonic generation during the rise time of the laser pulse. For frequencies high compared with the Kepler frequencies of the atoms, however, ionization suppression and stabilization in electric-field direction occurs with increasing laser-field intensity [11–21]. Experimental evidence for high-frequency stabilization is beginning to emerge [22].

Harmonic spectra of strongly accelerated electrons have been evaluated both quantum mechanically (see, e.g., Ref. [3], and references therein) and classically (see, e.g., Ref. [23], and references therein). For classical calculations single-electron trajectories can be determined for certain initial conditions of the coordinates and velocities in phase space. The quantum uncertainties can be simulated by averaging over a distribution of initial conditions. A microcanonical distribution has been employed in the Monte Carlo simulations, which have reproduced particularly successfully the interaction of highly excited states of hydrogen in an intense microwave field [23–27].

Most calculations have been performed nonrelativistically, as only recently have laser intensities become available that can accelerate the electron to relativistic velocities, although this problem was addressed some years ago [28]. This domain also appears interesting, as high accelerations of the electron sweeping through the nucleus promise higher orders of harmonics. It has been known for many years that even free electrons in relativistically strong laser fields can emit high multiples of the applied field, both from classical and quantum-mechanical evaluations [29–32]. When the interaction with the nucleus is included, the dynamics of the electron generally hardly changes in any significant way, provided the force of the laser field is much stronger than that of the nucleus [33]. In the relativistic harmonic spectrum, however, the presence of the nucleus becomes very important in the generation of high-order harmonics for those cases where the electron reverses its velocities close to the nucleus [34]. Earlier classical calculations in models of hydrogen had derived the relativistic working equations but did not explore the domain that is accessible today [35]. Recent quantum-mechanical calculations showed, to our knowledge, the first analytical relativistic evaluations of harmonic spectra by modeling the atom's binding potential by a δ function [36–38], and others have considered the effect of the electron spin in strong-field physics using the Dirac equation [39,40] and the Pauli equation [41]. The validity of the dipole approximation was shown to be acceptable in the nonrelativistic regime [41], while in the relativistic domain, violation of the dipole approximations with the consequent breakdown of stabilization has been pointed out [42].

In this paper we study the effects of a relativistically strong laser field on a hydrogen atom simulated by classical Monte Carlo techniques. The first effect is the role of

the acceleration of the electron to relativistic velocities by the electric-field component. In a previous preliminary study of the present authors [34] high harmonics were shown to emerge at times corresponding to the classical turning points where the electron suddenly reverses its velocity, which at these extrema is essentially the speed of light. This effect dominates in one-dimensional treatments or when the atom interacts with counterpropagating laser fields where the magnetic-field component is canceled at the point of maximal electric field. However, here we would like to emphasize the effect of the magnetic-field component of the laser field, which together with relativistic velocities in the polarization direction due to the electric-field component can induce significant velocities in the propagation direction. As a consequence, the essentially one-dimensional nonrelativistic motion of the electron is replaced by fully three-dimensional or at least essentially two-dimensional trajectories, and we have to expect much less significant interaction of the electron with the nucleus already for modestly relativistic laser intensities. For stronger intensities the problem of ionization in the propagation direction arises and is responsible for decreasing high harmonic generation. This effect can also be understood quantum mechanically as a consequence of the momentum transfer of the incoming photons due to multiple absorption and emission. In this formulation a possible breakdown of stabilization has been pointed out recently in a nonrelativistic approach [43]. To assist the survival of stabilization in the direction of propagation, we will also investigate the application of an additional laser field in the opposite direction.

The emitted electric field will be determined from the Lienard-Wiechert potential of a relativistically moving point charge [44] and is not usually simply propagation to the acceleration. The evolution of the electron in the propagation direction leads to Doppler shifts and broadening and in the case of crossed fields to dips in the spectrum at the nonshifted multiple resonance frequencies. This can be explained because every peak splits into two due to Doppler shifts in the two propagation directions of the counterpropagating fields. Throughout this paper we will identify harmonics as the multiples of the Doppler-shifted frequency, which can possibly differ significantly from the applied laser frequency. Retardation effects are included in the evaluations in the case of observation in the propagation direction and are neglected in the magnetic-field direction in the far-field approximation.

The dynamics of the atomic electron in the relativistically intense laser field is dominated by the laser field, so we devote the next section to the dynamics and radiation processes of a free electron in both single and counterpropagating (standing-wave) laser fields. The following section introduces the Monte Carlo simulations, where we model a real three-dimensional hydrogen atom with classical considerations. We then proceed with fully dimensional trajectories of the hydrogen electron and finally examine more closely the ionization rate, the breakdown of stabilization, excess photon ionization, and harmonic spectra.

II. FREE-ELECTRON TRAJECTORIES AND RADIATION

The central interest in this paper is in laser-field intensities above the atomic unit of intensity, which is equal to 3.5×10^{16} W cm^{-2}, and which corresponds to an electric-field atomic unit of 5.1×10^{9} V cm^{-1}, which is that sensed by the ground-state hydrogen electron (all units in this paper are atomic units if not specified otherwise). As the laser-field interaction then becomes dominant, it mainly controls the dynamics of the electron. This is why we would like to concentrate in this section on the dynamics of an unbound electron in a superstrong laser field. We will also determine the corresponding harmonic spectrum in order to show in later sections those features of the hydrogen spectra that arise solely from the relativistic motion of the free electron and those that are due to the interaction with the nucleus.

At this point we need to emphasize that the problem of a free electron in a laser of arbitrary strength has been solved analytically in many previous publications, e.g., [28–32], and a number of the results in this section have been given implicitly elsewhere. However, we believe it to be useful to present graphically the electron trajectories and spectra from the various observation directions for our particular choice of parameter domain in field strength, frequency, and pulse shapes. This enables us to obtain more insight into the nature of the atomic spectra presented in the following section for the same parameter domain.

We should give first some approximate expressions that describe at which laser-field intensities the problem becomes relativistic or in other words at which intensity the nonrelativistic treatment becomes invalid. We therefore consider the nonrelativistic classical equation of motion of an electron in a standing laser field $E=E_0\cos(\omega t)$:

$$m\ddot{x}(t)=eE_0\cos(\omega t)\ , \tag{1a}$$

$$\dot{x}(t)=\frac{eE_0}{m\omega}\sin(\omega t)\ , \tag{1b}$$

which shows that a relativistic treatment is necessary if

$$\frac{eE_0}{m\omega}\approx c\ , \tag{2a}$$

$$\frac{e^2E_0^2}{m\omega^2}\approx mc^2\ , \tag{2b}$$

i.e., when the electron velocity $\dot{x}$ becomes of the order of the speed of light c and its "quiver" kinetic energy approaches its rest mass energy mc^2. For convenience we will use atomic units in this paper, in which the electron mass m and charge e are set equal to 1 and c is 137, i.e., 137 times the velocity of the hydrogen electron in the ground-state orbit. The atomic unit of angular frequency ω is 4×10^{16} Hz corresponding to a wavelength of 45.6 nm. Thus for a typical laser field wavelength of 1 μm with an angular frequency 0.05 a.u. and an intensity of 3.5×10^{18} W cm^{-2} or an electric strength $E_0=10$ a.u., the ratio E_0/ω is of the order of 137 and we are clearly in

the relativistic domain. These are typical values we will use throughout this paper.

Our interest lies now in the relativistic time evolution of the electron in the laser field. In the beginning we concentrate purely on the influence of the electric-field component and imagine the electron in a standing laser field initially at rest at the point of maximal electric-field strength E_0 and vanishing magnetic field. In this case the evolution of the electron is one dimensional and the electron velocity obeys the equation of motion

$$m\frac{d}{dt}\frac{\dot{x}}{\sqrt{1-(\dot{x}/c)^2}}=eE_0\cos(\omega t)\ , \tag{3}$$

which can be solved to give

$$x(t)=x_0+\frac{c}{\omega}\arcsin\frac{R\cos(\omega t)}{\sqrt{1+R^2}} \tag{4a}$$

with a corresponding acceleration:

$$\ddot{x}(t)=\frac{(eE_0/m)\cos(\omega t)}{[1+R^2\sin^2(\omega t)]^{3/2}}\ . \tag{4b}$$

Here $R=eE_0/mc\omega$ is the ratio of the ponderomotive velocity to the speed of light, and is thus a measure of the relativistic feature of the problem, and x_0 accounts for the initial displacement of the electron.

The evolution of the free electron is displayed in Fig. 1 for various field strengths. The transition from a trigonometrical function at low intensities to a kinked function as the intensity increases is a clear relativistic feature and derives from the upper limit of the electron velocity of the speed of light c. In the nonrelativistic case, the electron can simply follow the sinusoidal evolution of the laser field up to any velocity, but in the relativistic case the motion becomes almost linear when the velocity of the electron approaches that of light. In this simple case, we can evaluate the radiation emitted at the sharp reversals of velocity by Fourier transforming the acceleration as given by Eq. 4(b). A typical spectrum is displayed in Fig. 2, showing in the logarithmic plot a linear reduction of the intensity of the odd harmonics with increasing order. This behavior can be reproduced approximately by Fourier transforming analytically the acceleration of Eq. 4(b) when the exponential factor that is really $\frac{3}{2}$ is replaced by 1. Under this rather drastic assumption one finds even harmonics vanishing, and for the odd harmonics the Fourier transform $\mathcal{F}$ reads

$$\mathcal{F}[(2n+1)\omega]=2\pi c\left\{\tan\left[\frac{1}{2}\arccos\left[\frac{1}{\sqrt{1+R^2}}\right]\right]\right\}^{2n+1}\ . \tag{5}$$

Taking the logarithm of the above expression we can compare the slope of Eq. (5) and that of Fig. 2 as a function of n and with

$$\ln[\tan(\tfrac{1}{2}\arccos\{1/\sqrt{1+[10/(0.05\times 137)]^2}\})]\approx -0.64\ ,$$

find quite reasonable agreement.

We now would like to investigate the time evolution of an electron in a propagating laser pulse. The equation of motion of the electron velocity is then determined by

$$m\frac{d}{dt}\frac{\dot{\mathbf{r}}}{\sqrt{1-(\dot{\mathbf{r}}/c)^2}}=eh(t)\mathbf{E}_0\cos(\omega t-\mathbf{k}\cdot\mathbf{r})$$

$$+\frac{e}{c}\dot{\mathbf{r}}\times h(t)\mathbf{H}_0\cos(\omega t-\mathbf{k}\cdot\mathbf{r})\ , \tag{6}$$

where $\dot{\mathbf{r}}$ denotes the velocity of the electron, $\mathbf{k}$ the propagation direction of the laser field, $\mathbf{E}_0$ and $\mathbf{H}_0$ the maximal electric- and magnetic-field vectors, respectively, with $|\mathbf{H}_0|=|\mathbf{E}_0|$, and the envelope function $h(t)$ is defined via

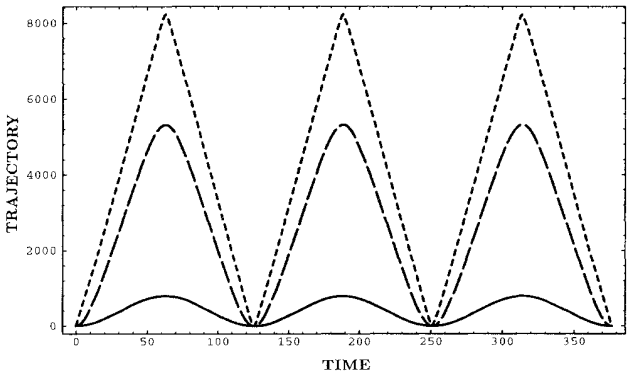

FIG. 1. Relativistic free-electron trajectories as a function of time in the polarization direction of a standing-wave laser field with angular frequency $\omega=0.05$ a.u., vanishing magnetic-field and electric-field strengths $E_0=1$ (solid line), 10 (long-dashed line), and 100 (short-dashed line) a.u. from the bottom to the top. These trajectories have been evaluated for a free electron but are hardly different for the hydrogenic electron trajectories for these field strengths. All units are in atomic units (a.u.).

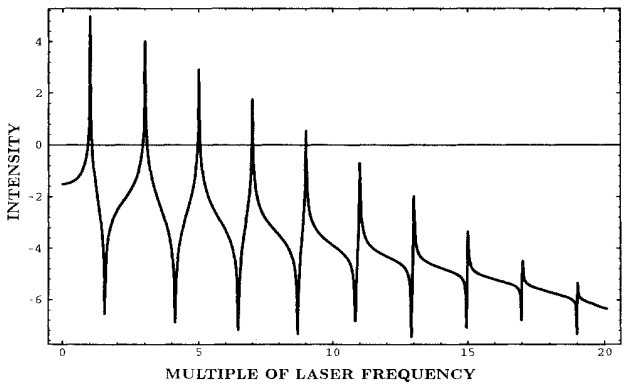

FIG. 2. Free-electron spectrum from an electron in a suddenly switched-on standing-wave field of electric strength 10 a.u. and frequency 0.05 a.u. The electron is assumed at rest initially at the point of vanishing magnetic field and the intensity spectrum (in arbitrary units) emitted perpendicular from the polarization direction is evaluated from the Fourier transform over 50 cycles of the acceleration in polarization direction. All units are in atomic units (a.u.).

$$h(t):=\begin{cases}\sin^2[\omega t/(4c_1)] & \text{if } 0<t<t_1:=2\pi c_1/\omega\ ,\\ 1 & \text{if } t_1<t<t_2:=2\pi c_2/\omega\ ,\\ \sin^2[\omega(t-t_2)/(4c_1)+\pi/2] & \text{if } t_2<t<t_2+t_{\cdot}\ ,\\ 0 & \text{otherwise}\ .\end{cases} \tag{7}$$

The symbols c_1 and c_2 denote the number of cycles for the turn-on phase and the number of remaining cycles until the beginning of the turnoff, respectively, which itself is assumed to be as long as the turn-on phase.

Before describing the electron trajectories we would like to define our three directions in space. The polarization direction is parallel to the electric-field component of the laser-field pulse, the magnetic-field direction to the magnetic component, and the forward direction to the direction of propagation of the laser pulse. A typical trajectory of an electron that encounters such a strong laser-field pulse is displayed in the parametric plot given in Fig. 3(a). It shows clearly the enormous momentum transfer of the photons to the electron in the direction of propagation, which will also be referred to as the forward direction. We therefore have to expect significant problems with ionization in the propagation direction, which will profoundly affect the atomic spectra as well as lead to the presence of Doppler shifts because the electron has a substantial velocity component in the direction of propagation. In fact, we can recognize from the electron trajectory in Fig. 3(a) that the electron hardly completes 40 cycles even though the field completed 50 in addition to five turn-on and five turn-off cycles. This means the electron acquires a speed in the propagation direction of $\frac{20}{60}=\frac{1}{3}$ of the velocity of light. We also have to consider retardation effects when we observe radiation in the forward direction.

The radiation of a relativistically moving point charge is well known from the Lienard-Wiechert potential [44]. In the far-field approximation the radiated electric field $\mathbf{E}_r(t)$ of the electron as detected by the observer at his time t is proportional to [44]

$$\mathbf{E}_r(t)\propto\frac{\mathbf{n}\times\left[\left[\mathbf{n}-\frac{\dot{\mathbf{r}}(t')}{c}\right]\times\ddot{\mathbf{r}}(t')\right]}{\left[1-\mathbf{n}\cdot\frac{\dot{\mathbf{r}}(t')}{c}\right]^3}\ . \tag{8}$$

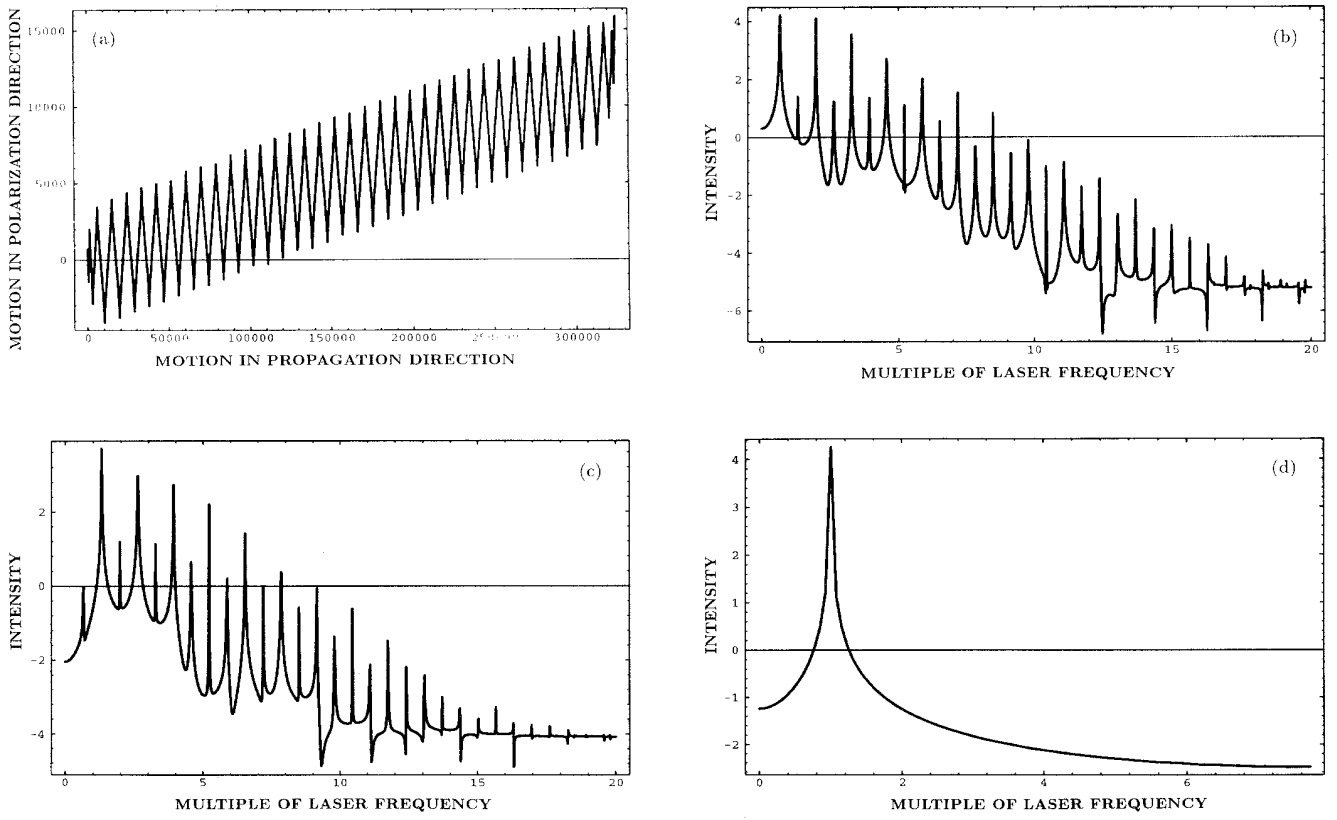

FIG. 3. (a) Parametric plot of the free-electron trajectory of the components in the polarization and propagation directions in a propagating laser pulse with $E_0=10$, $\omega=0.05$ a.u., number of turn-on and turn-off cycles $c_1=5$, and number of cycles at full amplitude $c_2=50$. In the other three figures the corresponding radiation spectra for far-field detection are displayed. The direction of observation in (b) and (c) is parallel to the magnetic-field component of the laser field and in (d) to the propagation direction of the laser pulse. (b) only displays the spectrum via the electric-field component in polarization direction and (c) the electric-field component in the propagation direction. All units are in atomic units (a.u.).

Here **n** defines the normalized observation direction and **r** the coordinate vector of the electron, to be evaluated at the retarded time t' of the electron. Choosing the magnetic-field direction as the observation direction **n**, we can neglect the retardation and the measured electric field is simply proportional to the acceleration of the electron. In the forward direction, say x, we have to evaluate for every measurement time t the retarded time t' via

$$t' - \frac{x[t']}{c} = t \ , \tag{9}$$

at which times the spatial, velocity, and acceleration components of the electron have to be determined to give the measured field at time t.

In Fig. 3(b) the far-field spectrum for the radiated electric field is displayed for the trajectory of Fig. 3(a) with the observation direction in the direction of the magnetic-field component of the laser field. This of course is hardly relevant to conventional harmonic-generation schemes, but does however emphasize the magnetic-field effects, because the drift of the electron in the forward direction manifests itself in the spectrum, which is measured perpendicular to its motion and thus not in the forward direction. As expected, we find a significant Doppler shifting of the fundamental and harmonics into the red since the electrons are moving with the field. The spectrum has only taken into account the electric-field component in the polarization direction of the applied field. Even harmonics are present, although these are strongly suppressed compared to the odd harmonics of the Doppler-shifted frequency. This can be explained by the fact that the motion of the electron in the polarization direction is partly influenced by the magnetic field, which destroys the center of inversion symmetry. An observation in the magnetic-field direction of the electric-field component in the direction of propagation of the applied field reveals the magnetic-field influence on the motion and shows even a dominance of even harmonics, though with a much smaller intensity than the radiation of components in the polarization direction [see Fig. 3(c)]. In the forward direction we in fact see only the fundamental as a discrete line, i.e., no harmonics are observable. In particular, there is no Doppler effect derived from the motion of the electron with the field. The electron of course also is affected by the Doppler-shifted frequency and emits multiples of this frequency in its rest frame, but the back transformation into the frame of a detector in the forward direction (direction of propagation of the beam) just reverses this effect. From a direction point of view, the presence of retardation for this direction of observation can also be made responsible for this effect. Magnetic-field effects are difficult to observe in the forward direction as the main effect of the magnetic field is to accelerate the electron in the direction of propagation and the radiation due to this motion is emitted perpendicular to its motion. It seems that the various contributions to the higher harmonics destructively interfere as changing the weighting of, e.g., the contributions in the acceleration in the polarization and propagation direction makes them reappear. If one includes the turn on and turn off of the electric field into the evaluation of the spectrum, the laser field deviates from a simple sinuisoid and some harmonics appear, including even ones.

III. IONIZATION PROBABILITY AND HARMONIC SPECTRA IN HYDROGEN

In this section we ill consider the full hydrogenic problem of the electron motion in both the relativistically strong laser field and the Coulomb field from the proton. We have seen [34] that the nonlinear interaction with the nucleus gives a significant boost to the high harmonic generation when the electron is strongly accelerated in its near vicinity. Our first concern, however, has to be to model the hydrogen atom itself. For our classical integration of the Lorentz equation, we need to compute the initial conditions of the electron in space and momentum. In a real atom, the electron wave function is distributed around the nucleus, obliging us to simulate this situation by averaging over various initial positions in space and momentum. This procedure employs a Monte Carlo simulation, is already well established [45,46], and has been utilized by numerous authors (e.g., [18,19,23,25, 26,35,45–47]). The applicability of this procedure compared to the exact quantum-mechanical computation has been analyzed, e.g., by Leopold and Percival [46]. In our calculations we have usually employed samples of several hundred up to more than a thousand members until we found that a further increase of trajectories does not lead to a visible change of the property under consideration. The averaging process to derive the initial conditions can be treated using entirely nonrelativistic dynamics because relativity enters the problem only when the superstrong laser field is applied to the atom. The nucleus alone accelerates the electron to velocities at most two orders of magnitude below that of the speed of light.

A. Monte Carlo simulations

The assumption of the classical Monte Carlo method is that the atom can be represented by an ensemble of electrons in a microcanonical distribution with an energy distribution function $\rho(\mathcal{E})$ given by

$$\rho(\mathcal{E}) \propto \delta(\mathcal{E} - \mathcal{E}_0) \ , \tag{10}$$

where $\mathcal{E}_0$ denotes the internal energy of the hydrogen atom. As the virial theorem applies to the Coulomb potential, the kinetic energy is $-\frac{1}{2}$ of the potential energy $V = -1/r$, leading us to set $\mathcal{E}_0 = -(0.5/n^2)$ a.u., with n being the principal quantum number. This amounts to randomly choosing Kepler orbits of the electron around the nucleus, as described by the Kepler equation [47]

$$\xi - \epsilon \sin[\xi] = \alpha \ , \tag{11}$$

where ξ, ϵ, and α denote the eccentric anomaly, eccentricity, and mean anomaly of the ellipse, respectively, and relate to the true anomaly via

$$\tan[\zeta/2] = \left[\frac{(1+\epsilon)}{(1-\epsilon)} \right]^{1/2} \tan[\xi/2] \ , \tag{12}$$

and to the angular momentum l and the absolute value of the displacement ρ from the nucleus and momentum $\not{k}$:

$$l=\sqrt{-\beta/(2U)}\ , \tag{13a}$$

$$\rho=\frac{\epsilon\cos[\xi]-1}{2U}\ , \tag{13b}$$

$$\not{k}^2=\frac{2m}{\rho}+\frac{\beta}{4U\rho^2}+U\ . \tag{13c}$$

The initial conditions of the various components of the displacements and velocities of the electron can then be expressed in terms of the Euler angles ϕ, ψ, and θ to give (e.g., [44])

$$r_x(0)=\rho(\cos[\phi]\cos[\psi+\zeta]-\sin[\phi]\cos[\theta]\sin[\psi+\zeta])\ , \tag{14a}$$

$$r_y(0)=\rho(\sin[\phi]\cos[\psi+\zeta]+\cos[\phi]\cos[\theta]\sin[\psi+\zeta])\ , \tag{14b}$$

$$r_z(0)=\rho(\sin[\theta]\sin[\psi+\zeta])\ . \tag{14c}$$

$$\dot{r}_x(0)=\frac{1}{\rho}\{\not{k}r_x(0)-l(\cos[\phi]\sin[\psi+\zeta]+\sin[\phi]\cos[\theta]\cos[\psi+\zeta])\}\ , \tag{15a}$$

$$\dot{r}_y(0)=\frac{1}{\rho}\{\not{k}r_y(0)-l(\sin[\phi]\sin[\psi+\zeta]-\cos[\phi]\cos[\theta]\cos[\psi+\zeta])\}\ , \tag{15b}$$

$$\dot{r}_z(0)=\frac{1}{\rho}\{\not{k}r_z(0)+l\sin[\theta]\cos[\psi+\zeta]\}\ . \tag{15c}$$

These initial conditions are then evaluated by randomly choosing $\cos[\theta]$, ϕ, ψ, α, and e^2 with equal probability in the range

$$-1\le\cos[\theta]\le 1,\quad 0\le\phi\le 2\pi,\quad 0\le\psi\le 2\pi\ , \tag{16a}$$

$$0\le\alpha\le\pi,\quad 0\le e^2\le 1\ . \tag{16b}$$

B. Breakdown of stabilization in the relativistic domain

In the following section we investigate the influence of the magnetic-field component on the trajectory of the electron around the nucleus with particular interest in the ionization rate. For this purpose we consider the equation of motion of the electron in the combined electric field of the laser, the magnetic field of the laser, and the Coulomb potential

$$m\frac{d}{dt}\frac{\dot{\mathbf{r}}}{\sqrt{1-(\dot{\mathbf{r}}/c)^2}}=eh(t)\mathbf{E}_0\cos(\omega t-\mathbf{k}\cdot\mathbf{r}+\phi)-\frac{e\mathbf{r}}{|\mathbf{r}|^3}+\frac{e}{c}\dot{\mathbf{r}}\times h(t)\mathbf{H}_0\cos(\omega t-\mathbf{k}\cdot\mathbf{r}+\phi)\ . \tag{17}$$

The influence of the magnetic-field component with amplitude perpendicular to the electric-field component and propagation direction and absolute value $|\mathbf{H}_0|=|\mathbf{E}_0|$ is to induce a motion in the propagation direction. This motion does not have direct consequences for the forward-direction spectrum because it induces radiation perpendicular to its motion. However, it separates the electron from the nucleus and reduces harmonics arising from this interaction. In Fig. 4(a) we have evaluated the mean distance of the electron after the laser pulse by averaging over the various trajectories, where we have compared the fully relativistic, fully nonrelativistic calculation and the case where just the magnetic-field strength was neglected. In the first case we find that the electron can be driven very far away from the nucleus after the laser pulse as soon as the relativistic momentum transfer in the forward direction becomes effective. In the two other cases without the magnetic-field component we have essentially one-dimensional trajectories and far lower separations from the nucleus for very strong fields. With increasing laser-field intensity, the electron acquires

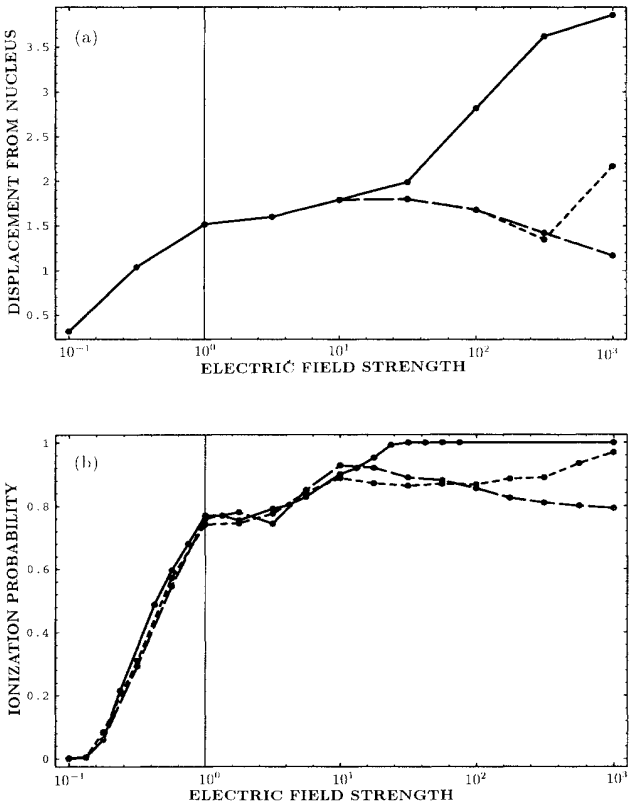

FIG. 4. Mean displacement of the electron from the nucleus (a) and ionization probability (b) as a function of the electric-field strength in a logarithmic plot after a laser pulse of ten cycles with $c_1=3$, $c_2=4$, a frequency of 1 a.u., and a Monte Carlo averaging over 500 trajectories. The solid line represents the relativistic evaluation, which takes into account the effect of the magnetic field, whereas the dashed is based on the neglect of the magnetic-field component of the laser field and the relativistic mass shift, i.e., is nonrelativistic. The curves with longer dashes represent the case where only the magnetic-field component has been neglected. The dots indicate at which points the calculation was performed. The plot shows that stabilization is removed due to ionization in the forward direction as a result of the magnetic-field component of the laser field. All units are in atomic units (a.u.).

higher velocities when passing by the nucleus, so that there is less time for the nucleus to disturb the periodic electron motion. This may explain the decrease observed in the displacement of the electron from the nucleus for a range of parameters with increasing laser intensity. In the completely nonrelativistic calculation, however, the electron can acquire extremely large velocities, which eventually results in an increasing mean displacement of the electron with rising laser-field intensity.

We have also considered the ionization probability by evaluating the energy of the electron after the laser pulse due to the expression

$$E_e = -\frac{e}{|\mathbf{r}|} + c\sqrt{m^2c^2+\mathbf{p}^2} - mc^2$$
$$= -\frac{e}{|\mathbf{r}|} + mc^2\left[\frac{1}{\sqrt{1-(\dot{\mathbf{r}}/c)^2}} - 1\right], \quad (18)$$

where $\mathbf{p}$ and $|\mathbf{r}|$ correspond to the momentum and displacement of the electron from the nucleus after the laser pulse, respectively. We count a trajectory as ionized when the energy E_e is larger than zero after the laser pulse [48]. We then consider many trajectories and define the ionization rate as the ratio of the number of ionized trajectories to the total number of considered trajectories. In the limit of a large number of trajectories the corresponding classical ionization rate can then be understood as an ionization probability, which is independent of the initial conditions [18,19,23–27]. In Fig. 4(b), we have evaluated the ionization probability as a function of the laser-field strength and note clearly that stabilization is inhibited by the magnetic component of the laser field. This result agrees with the recent Comment by Katsouleas and Mori [42], who put forward the possibility of a relativistic breakdown of stabilization. The work by Latinne, Joachain, and Dörr [41] is not concerned with these drastic effects because it considers the Pauli equation, which is essentially nonrelativistic, apart from an additional spin contribution. We have performed further investigations of the relativistic ionization rate for several high frequencies around 1 a.u. and in Fig. 5 for $\omega=5$ a.u. In all cases we find that the ionization probability approaches unity very quickly when the electron velocities approach that of light and the magnetic component of the laser field becomes effective. In the very-high-frequency case of five atomic frequency units in Fig. 5 it becomes apparent that stabilization does clearly occur in the classical three-dimensional Coulomb potential but then breaks down quickly when the momentum transfer of the incoming fields becomes too large to keep the electron from ionizing. However, the frequency required to generate this stabilization is higher than that which is expected from a quantum-mechanical evaluation, which predicts this phenomenon already for $w=1$. This unsatisfying feature was first pointed out in a nonrelativistic treatment by Gajda *et al.* [19] and was shown to be removed by smoothing the singular role of the nucleus by replacing the Coulomb potential by the so-called soft-core potential. This potential was introduced earlier to improve the accuracy of one-dimensional codes by Eberly, Su, and Javanainen [13,14]. The uncertainty relation

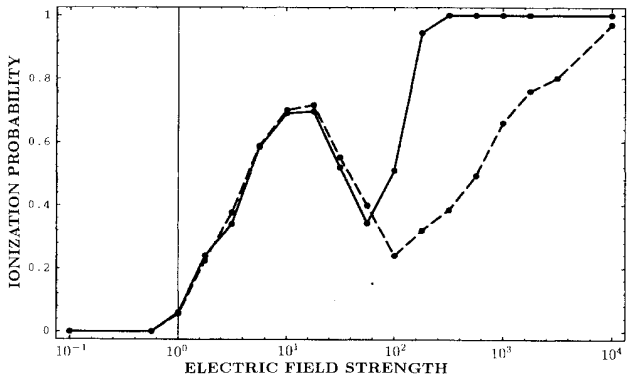

FIG. 5. Ionization probability as a function of the electric-field strength of the incoming laser light in a logarithmic plot for $w=5$ a.u. and all other parameters as in Fig. 4. In this very-high-frequency case the ionization rate displays clear stabilization between $E_0=10$ and 100 a.u. but approaches 1 again rapidly when the magnetic-field force becomes substantial. The dashed line describes the three-dimensional nonrelativistic case where the breakdown of stabilization is significantly slower. All units are in atomic units (a.u.).

allows us to understand how the electron avoids the nucleus in a quantum approach to atomic dynamics. This avoidance is not present in a classical approach, of course, but can be partly accounted for if a suitable smoothing operation is employed. We have already in a sense taken into account the consequences of the uncertainty relation for the electron by averaging over various trajectories so that it is sensible to assume the same for the nucleus. In Fig. 6 we have calculated the ionization probability of hydrogen in the soft-core potential $-e/\sqrt{|\mathbf{r}|^2+a^2}$ and indeed find stabilization for a laser frequency $w=1$ and a smoothing parameter $a^2=0.1$.

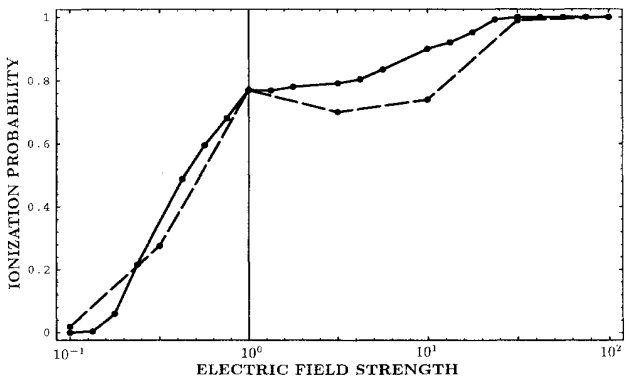

FIG. 6. Ionization probability as a function of the electric-field strength of the incoming laser light in a logarithmic plot for the parameters of Fig. 4. While the solid curve presents again the ionization rate of the Coulombic hydrogen atom, we have slightly smoothed the expectation value of the nucleus for the dashed curve by assuming the soft core potential with $a=0.1$. We now find agreement of the stabilization with quantum-mechanical calculations that also predict stabilization for this frequency. All units are in atomic units (a.u.).

C. Excess photon ionization

In the preceding section we were interested in the ionization probability, i.e., in the question of whether the electron is bound or free after the laser pulse and thus if the energy after the pulse is below or above zero. At this point we turn to the question of the energy distribution of the electron because only a highly energetic electron is capable of emitting high harmonics. For this purpose we consider again Eq. (17), which describes the dynamics of the motion, and at the end of the pulse we evaluate the total energy of the electron according to Eq. (18). We have again concentrated our attention on high frequencies, because those have more likelihood for stabilization and seem more promising to generate harmonics due to the interactions with the nucleus. In Fig. 7(a) we have displayed the energy distribution of the electron after a short pulse of ten cycles, for laser field strengths similar to the field strength of the nucleus. We find that the peak of the distribution just crosses the threshold at those intensities, i.e., here the most likely energy of the electron is just equal to its rest mass. Moreover, we observe that the distribution spreads while the peak moves to higher energies with increasing laser-field strength. This could explain why the ionization probability does increase rather slowly when the field strengths of the nucleus and laser field become comparable.

In Fig. 7(b) we considered the excess photon ionization for intensities that accelerate the electron to relativistic velocities. For those intensities we note that the electron starts to absorb significant amounts of energy. However, this is mainly due to the relativistic motion of the electron on its own and not due to the interaction with the nucleus, i.e., the energy distribution would be rather similar for a free electron in a laser field with the same initial electronic distribution in space and momentum but without the central nucleus. In addition we have seen in the preceding section for the free electron that this energy is not emitted as high harmonics in the forward direction. We conclude from the breakdown of stabilization for relativistic driving intensities and from the rather low

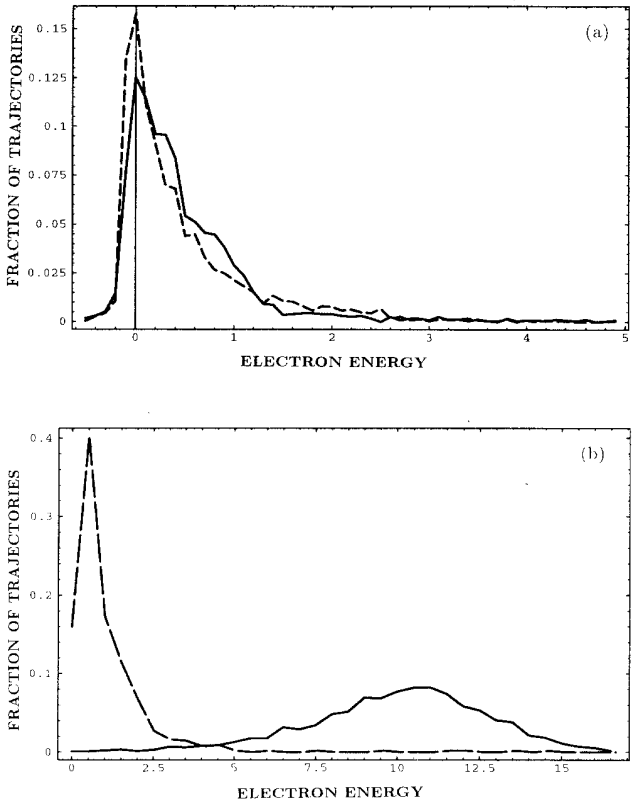

FIG. 7. Excess photon ionization represented by the fraction of trajectories, which corresponds to a certain electron energy after the laser pulse of ten cycles ($c_1=3$, $c_2=4$) and frequency $w=1$ a.u. In (a) the dashed line corresponds to $E_0=10^{0.25}$ a.u. and the solid line to $E_0=10^{0.75}$ a.u.; and in (b) the dashed line corresponds to $E_0=10^{1.875}$ a.u. and the solid line to $E_0=10^2$ a.u. While (a) shows the regime when the excess photon ionization peak of the energy distribution crosses the threshold for ionization, (b) considers the case when the electron reaches high energies in the relativistic range of electron velocities. All units are in atomic units (a.u.).

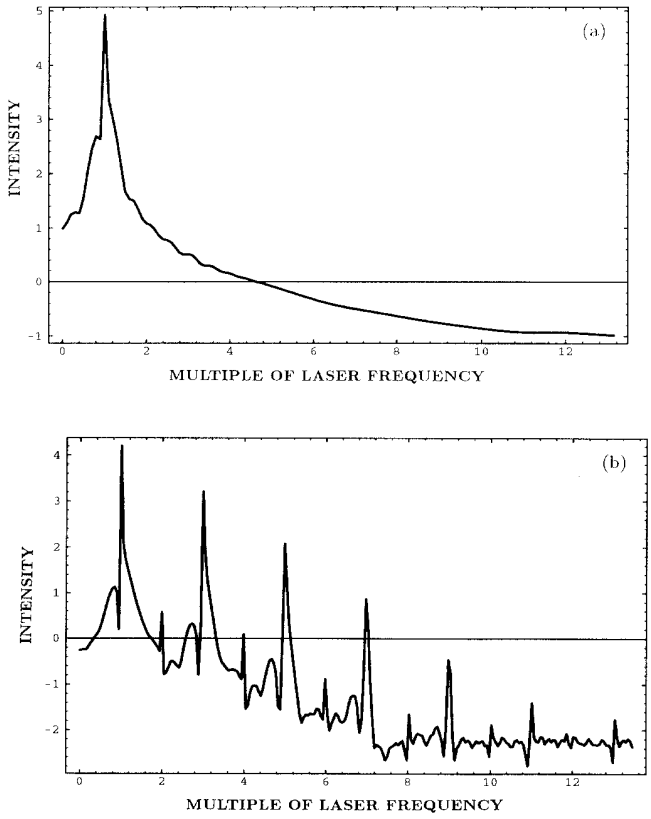

FIG. 8. (a) Monte Carlo averaged atomic spectrum in the forward direction for the situation for hydrogen in a propagating laser pulse with $E_0=10$, $\omega=0.05$ a.u., $c_1=3$, $c_2=17$, a detection time of ten cycles, and the number of orbits 50. The spectrum considers the electric-field component in the polarization direction of the radiation in the forward direction. It also takes into account the turn on of the laser field as the electron rapidly ionizes. (b) represents the spectrum for the corresponding case without the magnetic-field component. All units are in atomic units (a.u.)

amounts of energy, which the electron absorb under the influence of the laser field, that high harmonic generation should not occur for relativistic driving intensities. Moreover, we note that the electron begins to acquire large amounts of energy in a range of parameters where the ratio of the electric-field strength to the laser-field frequency is of the order of $E_0/\omega = 100$. This is just in the region where the dynamics becomes relativistic and where we also find a strong reduction in stabilization. Since by then the electrons are mostly unbound, these high energies can hardly come from the interaction with the nucleus. Therefore they are more likely to arise directly from the high relativistic acceleration of the almost free electron in the laser field. Furthermore, we need to point out that relativity has a crucial effect already in the modestly relativistic range of parameters where stabilization is still present. Well before the breakdown of stabilization the magnetic-field component of the laser field turns the essentially one-dimensional trajectory of the electron into a three-dimensional trajectory. This motion in the two other dimensions could be very small and without significant influence on the ionization rate, but can, however, be of great importance of the high harmonic generation. The electric-field component of the laser field induces a wiggling of the electron in the polarization direction that would pass the electron very close to the nucleus in the case of a vanishing magnetic field. Even a small magnetic field, however, could induce some displacement of the electron in, e.g., the propagation direction, with the consequence that the interaction with the nucleus is substantially reduced when the electron passes through the point where its component in the polarization direction is identical to that of the nucleus. In the following sections we will investigate the radiation spectrum in some more detail.

D. Atomic spectra in a single propagating laser field

We now turn our attention to the study of the radiation spectrum of hydrogen interacting with a single propagating laser field. The equation of motion of the electron in the laser and Coulombic binding field is hereby given again by Eq. (17). We have found no significant influence of small smoothing on the harmonic generation in the relativistic domain and have continued using the Coulomb potential. Solving this equation numerically we obtain the trajectory of the electron as well as its velocity and acceleration as a function of the time as measured in the frame of the electron. For relativistic values of the electric-field strength and frequency we obtain trajectories which are very similar to those of a free electron in a laser field as shown in Fig. 3(a). The strong "radiation pressure" leads to almost immediate ionization. The field as measured by the detector can then be determined via Eq. (8) where major numerical complications are introduced because the expression in Eq. (8) has to be evaluated at the retarded time. This includes an inversion of the position of the trajectory as a function of time. In Fig. 8(a) we find the resulting spectrum of hydrogen in the presence of a highly relativistic laser field at intensity of ca. 10^{18} W cm^{-2} and wavelength of 1 μm. As a result of the almost immediate ionization we detect essentially only the fundamental frequency in the harmonic spectra. In order to see the important influence of the magnetic field, in Fig. 8(b) this component has been ignored for the computation of this figure (which of course is incorrect) and therefore the strong motion of the electron in the forward direction is absent. This increases the interaction of the electron with the nucleus but the main contribution to the harmonic output arises from the now disturbed cancellation of the various relativistic effects.

E. Atomic spectra in a standing laser field

In this section we solve the classical equation of motion of the electron in two oppositely directed electromagnetic fields and in the Coulomb potential of the nucleus as governed by the equation of motion:

$$m\frac{d}{dt}\frac{\dot{\mathbf{r}}}{\sqrt{1-(\dot{\mathbf{r}}/c)^2}} = e\left[h(t)\mathbf{E}_0[\cos(\omega t-\mathbf{k}\cdot\mathbf{r}+\phi)+\cos(\omega t+\mathbf{k}\cdot\mathbf{r}+\phi)]-\frac{e\mathbf{r}}{|\mathbf{r}|^3}\right] + \frac{e}{c}\dot{\mathbf{r}}\times h(t)\mathbf{H}_0[\cos(\omega t-\mathbf{k}\cdot\mathbf{r}+\phi)+\cos(\omega t+\mathbf{k}\cdot\mathbf{r}+\phi)] . \tag{19}$$

The advantage of the use of a standing laser field is that the motion of the electron in the propagation direction is also affected by momentum transfer of a laser field encountering the electron from the opposite direction. The momentum transfer in the propagation direction in counterpropagating fields can be understood by considering the acceleration of the electron in the propagation direction x:

$$\ddot{x}(t) = \left[1-\frac{\dot{\mathbf{r}}(t)^2}{c^2}\right]^{1/2} h(t)|\mathbf{H}_0|\frac{\dot{y}(t)}{c}\left[\cos\left[-\omega t+\frac{\omega}{c}x(t)\right]-\cos\left[\omega t+\frac{\omega}{c}x(t)\right]\right]$$
$$= 2\left[1-\frac{\dot{x}(t)^2+\dot{y}(t)^2+\dot{z}(t)^2}{c^2}\right]^{1/2} h(t)|\mathbf{H}_0|\frac{\dot{y}(t)}{c}\sin(\omega t)\sin\left[\frac{\omega}{c}x(t)\right] , \tag{20}$$

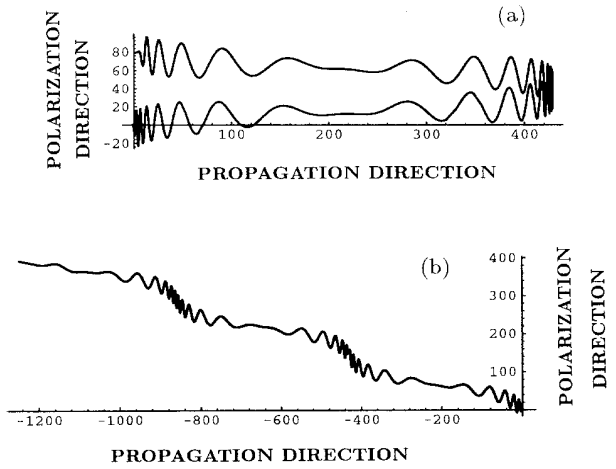

FIG. 9. Projection of three-dimensional trajectories of a bound electron in counterpropagating laser fields with $E_0=10$, $\omega=1$ a.u., $c_1=2$, $c_2=28$ on the plane spanned by the propagation direction of the counterpropagating identical laser pulses and the equal polarization direction of the two laser fields. The chosen initial conditions for the electron are (a) displacement from nucleus by 1 a.u. in the negative direction of the polarization direction of the laser fields ($d_y=-1$) and a velocity of 1 a.u. in the positive propagation direction ($v_x=1$); and in (b) with modified initial conditions $d_y=1$, $v_x=-1$, and all other dynamical variables were assumed to be equal to zero in both cases. The electron always slows down at the point of vanishing total magnetic field but the actual reflection depends strongly on the initial conditions. All units are in atomic units (a.u.).

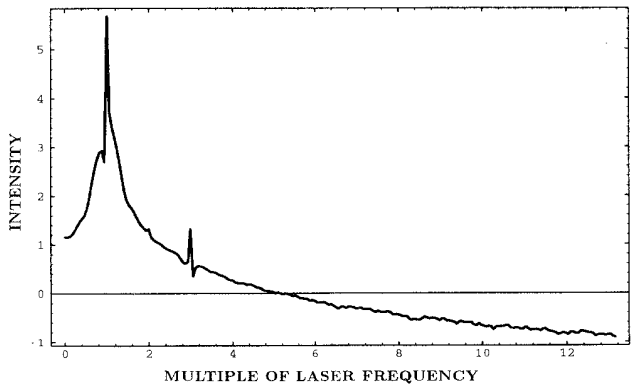

FIG. 10. Monte Carlo averaged atomic spectrum in the forward direction for the situation in Fig. 8 with $E_0=10$, $\omega=1$ a.u., $c_1=3$, $c_2=17$, and the number of orbits at 100. The spectrum considers the electric-field component in the polarization direction of the radiation in the forward direction. It also takes into account the turn on of the laser field as the electron rapidly ionizes. Due to the presence of counterpropagating laser fields the electron may return in the propagation direction, but the likelihood of passing the nucleus closely is however very small in three dimensions. All units are in atomic units (a.u.).

where y and z correspond to the components of the electron trajectory in polarization and magnetic-field direction. Whenever the term $(\omega/c)x(t)$ reaches the value π, the acceleration in the propagation direction reverses its sign and may make the electron return, depending on the remaining momentum at this point. We also see that these reversals occur earlier for higher frequencies, in agreement with stabilization in the polarization direction. In Fig. 9 we have displayed two typical trajectories of an electron in a counterpropagating laser field where the electron is reflected at the point of vanishing magnetic field, or just slowed down to almost vanishing velocity. However, in this three-dimensional consideration, the probability that the electron crosses the value zero in x simultaneously with small values in the coordinates y and z is very small. Due to this increase in phase space the interaction with the nucleus is rather weak and as a consequence the harmonic generation only shows very few harmonics, as is visible in Fig. 10. We note a relatively wide structure of the fundamental and the presence of a third harmonic. The even harmonic is rather small because symmetry is reestablished due to the presence of the counterpropagating second laser field.

In our fully relativistic treatment of one single atom in a standing laser field we have seen that the electron is strongly accelerated at the nodes of the magnetic-field component of the laser field, while it has a very large velocity in between these regions. This model does not include the interaction with other atoms so that the distance among neighboring atoms needs be larger than the distance between those nodes of vanishing magnetic fields, i.e., the wavelength of the applied laser field. However, we can conjecture enhanced harmonic generation in multiatom systems when the distance among these nodes is roughly equal to the separation of neighboring atoms (or to a smaller degree if one is an integer multiple of the other). Then the electron would be strongly accelerated in the vicinity of a nucleus, which as shown in Ref. [34] leads to pronounced high harmonic generation. Such a situation could be realized in a lattice where the wavelength (i.e., $\pi c/w$) of the laser field is an integer multiple of the distance among the neighboring atoms. For the choice of parameters for Fig. 9 this wavelength and therefore the most favorable distance among atoms is $\pi 137$ a.u. ≈ 430.4 times the Bohr radius.

IV. CONCLUSION

We have found that the magnetic-field component of the laser field may induce a significant motion of the electron in the propagation direction of the laser field. This adds an extra two dimensions in the trajectories of the electron and leads, even in the stabilization regime, to less interaction with the nucleus and in the strong relativistic regime to ionization and a breakdown of stabilization. As a consequence we find very few harmonics in the radiation spectrum. We moreover have emphasized the importance of the observation direction and have pointed out here that Doppler shifts occur for an observation perpendicular to the propagation direction of the laser field and that the various relativistic effects such as Doppler shifting and retardation cancel out each other in the detected spectrum in the forward direction.

ACKNOWLEDGMENTS

The authors gratefully acknowledge helpful discussions with K. Burnett, J.-P. Connerade, M. H. R. Hutchinson, A. Maquet, M. Protopapas, D. Richards, and C. Szymanowski, and financial support by the European Community and the U.K. Engineering and Physical Sciences Research Council.

[1] G. H. C. New and J. F. Ward, Phys. Rev. Lett. **19**, 556 (1967).
[2] B. W. Shore and P. L. Knight, J. Phys. B **24**, 325 (1987).
[3] A. L'Huillier, L. A. Lompre, G. Mainfray, and C. Manus, *Advances in Atomic, Molecular and Optical Physics,* edited by M. Gavrila (Academic, New York, 1992).
[4] The whole field of superintense field-atom interactions is reviewed in *Atoms in Intense Laser Fields,* edited by M. Gavrila (Academic, Boston, 1992).
[5] K. Burnett, V. C. Reed, and P. L. Knight, J. Phys. B **26**, 561 (1993).
[6] A. L'Huillier and P. Balcou, Phys. Rev. Lett. **70**, 774 (1993).
[7] J. J. Macklin, J. D. Kmetic, and C. L. Gordon III, Phys. Rev. Lett. **70**, 766 (1993).
[8] J. Tisch, R. Smith, J. Muffett, M. Ciarocca, J. Marangos, and M. H. R. Hutchinson, Phys. Rev. A **48**, R28 (1994).
[9] M. D. Perry and J. K. Crane, Phys. Rev. A **48**, R4051 (1993); and private communication.
[10] P. B. Corkum, Phys. Rev. Lett. **71**, 1994 (1993).
[11] M. Gavrila, in *Atoms in Super-Intense Fields,* edited by M. Gavrila (Academic, Boston, 1992).
[12] M. H. Mittleman, Phys. Rev. A **29**, 2245 (1984).
[13] J. H. Eberly, Q. Su, and J. Javanainen, Phys. Rev. Lett. **62**, 881 (1989).
[14] Q. Su, J. H. Eberly, and J. Javanainen, Phys. Rev. Lett. **64**, 862 (1990).
[15] V. C. Reed, P. L. Knight, and K. Burnett, Phys. Rev. Lett. **67**, 1415 (1991).
[16] V. C. Reed, K. Burnett, and P. L. Knight, Phys. Rev. A **47**, R34 (1993).
[17] P. L. Knight, M. Protopapas, C. Keitel, S. Vivirito, K. Burnett, V. C. Reed, and S. C. Rae, in *Super-Intense Laser-Atom Physics,* Vol. 316 of *NATO Advanced Study Institute Series, B: Physics,* edited by B. Piraux, A. L'Huillier, and K. Rzazewski (Plenum, New York, 1993).
[18] J. Grochmalicki, M. Lewenstein, and K. Rzazewski, Phys. Rev. Lett. **66**, 1038 (1991).
[19] M. Gajda, J. Grochmalicki, M. Lewenstein, and K. Rzazewski, Phys. Rev. A **46**, 1638 (1992).
[20] J. Bestle, V. A. Akulin, and W. P. Schleich, Phys. Rev. A **48**, 746 (1993).
[21] K. C. Kulander, K. J. Schafer, and J. L. Krause, Phys. Rev. Lett. **66**, 2601 (1992).
[22] M. P. de Boer, J. H. Hoogenraad, R. B. Vrijen, L. D. Noordam, and H. G. Muller, Phys. Rev. Lett. **71**, 3263 (1993).
[23] G. Bandarage, A. Maquet, T. Menis, R. Taieb, V. Veniard, and J. Cooper, Phys. Rev. A **46**, 380 (1992).
[24] J. E. Bayfield and P. M. Koch, Phys. Rev. Lett. **33**, 258 (1974).
[25] I. C. Percival and D. Richards, At. Mol. Phys. **11**, 1 (1975); J. G. Leopold and I. C. Percival, J. Phys. B **12**, 709 (1979).
[26] D. Richards, J. G. Jensen, P. M. Koch, E. J. Galvez, K. A. H. van Leeuven, L. Moorman, B. E. Sauer, and R. V. Jensen, J. Phys. B **22**, 1307 (1989).
[27] B. E. Sauer, S. Yoakum, L. Moorman, P. M. Koch, D. Richards, and P. A. Dando, Phys. Rev. Lett. **68**, 468 (1992).
[28] J. H. Eberly, Prog. Opt. **7**, 359 (1969).
[29] A. Sarachik and E. S. Schappert, Phys. Rev. D **1**, 2738 (1970).
[30] L. S. Brown and T. W. B. Kibble, Phys. Rev. **133**, A705 (1964).
[31] T. W. B. Kibble, in *Lectures in Physics,* edited by M. Levy (Gordon and Breach, New York, 1968), p. 299.
[32] J. H. Eberly and A. Sleeper, Phys. Rev. **176**, 1570 (1968).
[33] J. Grochmalicki, M. Lewenstein, M. Wilkens, and K. Rzazewski, J. Opt. Soc. Am. B **7**, 607 (1990).
[34] C. H. Keitel, P. L. Knight, and K. Burnett, Euro. Phys. Lett. **24**, 539 (1993).
[35] G. A. Kyrala, J. Opt. Soc. Am. B **4**, 731 (1987).
[36] F. H. M. Faisal and T. Radozycki, Phys. Rev. A **47**, 4464 (1993).
[37] F. H. M. Faisal and T. Radozycki, Phys. Rev. A **48**, 554 (1993).
[38] W. Becker, S. Long, and J. K. McIver, Phys. Rev. A **41**, 4112 (1990).
[39] J. Z. Kaminski, Z. Phys. D **16**, 153 (1990).
[40] P. Krstic and M. H. Mittleman, Phys. Rev. A **45**, 6514 (1992).
[41] O. Latinne, C. J. Joachain, and M. Dörr, Europhys. Lett. **26**, 333 (1994).
[42] T. Katsouleas and W. B. Mori, Phys. Rev. Lett. **70**, 1561 (1993).
[43] A. Bugacov, M. Pont, and R. Shakeshaft, Phys. Rev. A **48**, R4027 (1993).
[44] L. Landau and L. Lifshitz, *The Classical Theory of Fields,* 2nd ed. (Addison-Wesley, Reading, MA, 1951).
[45] R. Abrines and I. C. Percival, Proc. Phys. Soc. **88**, 861 (1966).
[46] J. G. Leopold and I. C. Percival, J. Phys. B **12**, 709 (1979).
[47] G. Bandarage and R. Parson, Phys. Rev. A **41**, 5878 (1990).
[48] J. H. Eberly, in *Atoms in Super-Intense Fields* (Ref. [11]).